

Effects of β^- -Emitting ^{188}Re Balloon in Stented Porcine Coronary Arteries

An Angiographic, Intravascular Ultrasound, and Histomorphometric Study

Raj Makkar, MD; James Whiting, PhD; Alex Li, PhD; Hidehiko Honda, MD;
Michael C. Fishbein, MD; F.F. (Russ) Knapp, PhD; Jörg Hausleiter, MD;
Frank Litvack, MD; Neal L. Eigler, MD

Background—Restenosis within stents may be prevented by ionizing radiation from an intravascular source.

Methods and Results—A liquid β^- radiation (^{188}Re) balloon was evaluated in a randomized and blinded porcine coronary model of stent restenosis. Group A pigs (n=17) received 0.16, 22, or 29 Gy at 0.5-mm depth, followed by stenting. Restenosis was quantified by angiography, ultrasound, and histomorphometry at 30 days. Group B (n=7) was stented first and then treated with 0 or 29 Gy with follow-up at 60 days. There was a measurable effect at 16 Gy, which improved with increasing doses. At 29 Gy, the histological stenotic area was reduced by 67% (22% versus 66% in controls, $P<0.001$). Radiation after stenting was equally effective: the stenotic area was reduced (21% versus 65%, $P<0.001$). At 16 Gy, the vessel just distal to the stent was significantly smaller than control vessels because of intimal thickening ($P=0.003$). Radiated vessels had distinctive histology consisting of neointimal fibrin and reduced smooth muscle cells and matrix ($P<0.0001$).

Conclusions— ^{188}Re balloon brachytherapy in porcine coronary arteries results in dose-dependent and injury-independent inhibition of stent restenosis for up to 60 days. Restenosis at the borders of the irradiated zone is a potential limitation and may be related to underdosing. Brachytherapy with the ^{188}Re balloon appears to be safe and feasible for clinical studies. (*Circulation*. 2000;102:3117-3123.)

Key Words: balloon ■ restenosis ■ angioplasty ■ stents

Restenosis within stents has high rates of recurrence and morbidity.¹ Restenosis may be prevented by ionizing radiation delivered from an intravascular source. A variety of devices and sources, including radionuclide-coated stents and catheters containing radioactive wires or seeds, are being developed. This report describes the initial experience with a β^- -emitting liquid-filled ^{188}Re balloon in a porcine model of coronary stenting. The effects of dose, stent attenuation, location with respect to the irradiated field, and duration of effect up to 2 months were examined by quantitative angiography (QCA), intravascular ultrasound (IVUS), and histology.

Methods

Radiation Delivery System

The radiation delivery system (Radiant, US Surgical, Inc) (Figure 1) consisted of a balloon catheter coupled to a liquid radiation source contained in a shielded isolation and transfer device (ISAT). The catheters were modified rapid-exchange-type polyethylene PTCA

balloons with dual radiopaque markers, puncture resistant walls, and self-sealing connectors. Balloons achieved nominal diameter at 3 atm.

Sterile ^{188}Re perrhenate (NaReO_4) with activity concentrations ranging from 50 to 150 mCi/mL was produced by eluting a ^{188}W - ^{188}Re generator (Oak Ridge National Laboratory). The half-life is 17 hours, and the maximum β^- energy is 2.1 MeV. γ emissions (16%) facilitate calibration and leak detection while contributing a negligible dose to the arterial wall.

The ISAT contains a smaller syringe filled with isotope coupled to the balloon by redundant self-sealing connectors. A 1-cm-thick leaded acrylic shield surrounds the isotope. The isotope syringe plunger is coupled back to back with the plunger of a saline-containing syringe that, in turn, is connected to a standard PTCA inflation device by 30-in tubing and a pressure-limiting (4-atm) valve. Operation of the inflation device transfers the isotope between ISAT and the balloon.

Treatment time depends on the prescribed dose at 0.5 mm radial to the balloon surface, balloon diameter, isotope activity concentration, and isotope decay. Negligible radiation is delivered during balloon deflation. Thus, the balloon can be cycled as many times as necessary to deliver the dose permitting intermittent perfusion. Dose to the operator is limited to bremsstrahlung and γ emissions.

Received November 23, 1999; revision received July 11, 2000; accepted July 13, 2000.

From the Division of Cardiology and the Research Institute at Cedars-Sinai Medical Center and the UCLA School of Medicine (R.M., H.H., J.H., F.L., N.L.E.), the Division of Medical Physics at Cedars-Sinai Medical Center (J.W., A.L.), and the Department of Pathology at UCLA School of Medicine (M.C.F.), Los Angeles, Calif, and the Oak Ridge National Laboratory (F.F.K.), Oak Ridge, Tenn.

Correspondence to Neal Eigler, MD, Cedars-Sinai Medical Center, 8700 Beverly Blvd, Los Angeles, CA 90048. E-mail IB1surfdoc@aol.com
© 2000 American Heart Association, Inc.

Circulation is available at <http://www.circulationaha.org>

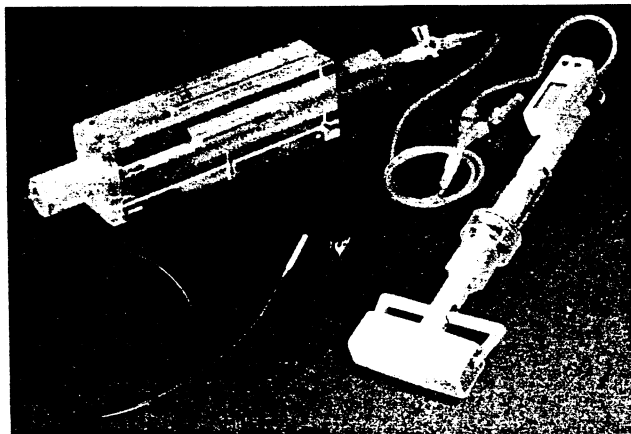


Figure 1. ^{188}Re balloon (Radiant) brachytherapy system, involving (left to right) rapid-exchange balloon, shielded ISAT, over-pressure relief valve, and commercial PTCA inflation device.

Figure 2 shows isotope depth-dose plots for the long axis of the balloon. Without a stent, the radiation fields are highly uniform at depths from contact to 2.0 mm. When stents are positioned over the balloon, a pattern of strut attenuation creates shadows that are visible at contact but are absent at 0.5-mm depth.

Study Design

The Institutional Animal Care and Use Committee approved the experiments. Group A was involved in a dose-response study in which arteries were irradiated before stenting. Juvenile farm pigs ($n=17$, 25 to 30 kg) received 250 mg ticlopidine and 325 mg aspirin the day before and for 7 and 30 days thereafter, respectively.

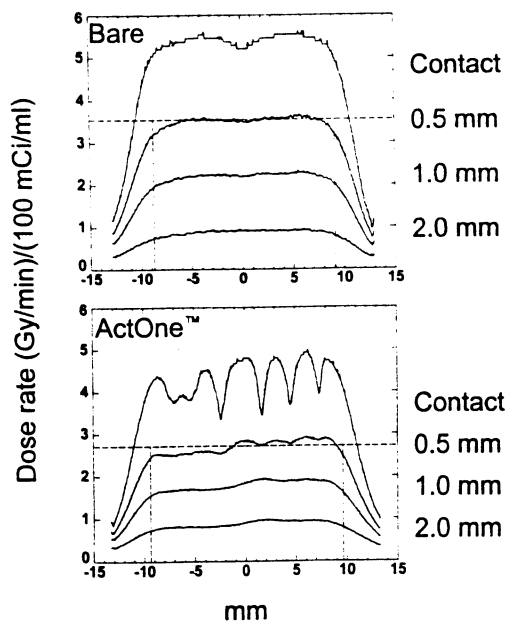


Figure 2. Dose-rate profiles at contact and 0.5-, 1.0-, and 2.0-mm radial distance along 3.0×20-mm Radiant balloon or balloon plus stent, measured with use of Gafchromic film. Horizontal dashed line is mean dose in center third of balloon at 0.5-mm depth. Vertical dashed lines are distances from balloon center, where dose rate falls off by 10% from central dose. Top, bare balloon. Dose rate is uniform except for small surface "cold spot" detected at contact correlating with a small air bubble in balloon. Bottom, Dose-rate profile with ACT-One stent in place. ACT-One stent used in animal studies reduced dose by 21%.

Anesthesia was maintained with isoflurane, followed by 5 mg/kg bretylium and 10 000 IU heparin intravenously. Coronary angiograms were performed after 200 μg IC nitroglycerin.

Segments of the right coronary artery (RCA) and left anterior descending coronary artery (LAD) were irradiated with 3.5×20-mm balloons. Arteries were randomized to receive 0, 16, 22, or 29 Gy. One-minute inflation/deflation cycles were performed until the prescribed dose was administered. Balloon-vessel contact was confirmed by contrast injection. Blood samples were assayed for radioactive contamination. All study participants except the physicist (A.L.) were blinded to dose until the completion of data analysis.

A 4.0×17-mm nitinol stent (ACT-One, US Surgical, Inc) was deployed at 12 atm within the irradiated segment. At 30 days, QCA and IVUS were performed, followed by euthanasia under general anesthesia. The coronary arteries were perfusion-fixed and placed in formalin.

Of the 34 coronary arteries attempted, 1 RCA could not be cannulated with a guide catheter, and 1 LAD could not be successfully stented. One LAD receiving 22 Gy was occluded at follow-up. The results are included, but IVUS examination was not possible. Histology revealed organized occlusive stent thrombosis.

Group B was involved in irradiation after stent placement; follow-up was extended to 60 days. Pigs ($n=7$) received a 3.5×17-mm ACT-One stent, followed by irradiation with 0 or 29 Gy. Otherwise, the methodology was identical to that for group A. One irradiated LAD was excluded because the stent migrated 10 mm proximal to the treated segment immediately after radiation delivery. A single additional pig was euthanized at 2 days to observe the early effects of brachytherapy.

Data Acquisition and Analysis

QCA parameters included the following: proximal and distal reference diameters, minimum lumen diameter (MLD) and mean lumen diameter, minimum and mean percent diameter stenosis, and mean and maximal late loss. Ten IVUS frames (6 within the stent and 2 in the 5-mm segments proximal and distal to the stent) were selected at 2.5-mm intervals for planimetry. Measurements included stent, lumen, and intimal areas. Tissue blocks were embedded in methyl methacrylate and cut into 4 cross sections at predetermined points to avoid sampling bias. From proximal to distal, sections were taken at 2, 6, 9, and 15 mm within the stent. Stained sections (paragon stain)² were evaluated by an experienced cardiovascular pathologist (M.C.F.). Table 1 summarizes prospectively defined grades for intimal, medial, and adventitial features. The circumferential extent of media disrupted or absent was measured. The appearance of the vasa vasorum and myocardium surrounding the artery were also systematically evaluated. Histological sections were scanned at 9- μm resolution for automatic edge detection and measurement of the areas constituting the lumen, boundary of the stent struts, and neointimal thickness. Percent area stenosis was calculated as $100 \times (\text{stent area} - \text{lumen area}) / \text{stent area}$. The mean injury score was measured as described by Schwartz et al.³

Statistical Analysis

Data are summarized as mean \pm SD. Comparisons were by ANOVA and by ANCOVA, where the covariate variable was the injury score. Post hoc testing was by the least significant difference method. Comparison between ranks was by Kruskal-Wallis ANOVA. At $P < 0.05$, post hoc comparisons were by the Mann-Whitney U test corrected for multiple comparisons. Comparisons for nominal-scaled data were by χ^2 analysis or by the Fisher exact test. Relationships between variables were assessed by linear regression or by Spearman rank correlation.

Results

Irradiation Before Stenting

There were no radiation leaks. The total exposure outside the operator's lead apron, exclusive of fluoroscopy, was < 1 mR per treatment. Table 2 summarizes the quantitative results for

TABLE 1. Prospective Definitions for Grading of Histological Features

	Grade			
	0	1	2	3
Extracellular matrix	None	Focal separation of SMCs by acellular pink-staining material	Regional full thickness separation of SMCs	Circumferential separation of SMCs
Inflammation	None to rare lymphocyte or macrophage seen on high power	Few lymphocytes or macrophages seen at high power	Focal areas of increased cellularity visible on low power	Circumferential increased cellularity visible at low power
Foreign body reaction	None	Occasional giant cell in proximity to strut	Multiple struts with focal accumulation of giant cells	Multiple struts surrounded by giant cells
Fibrinoid deposits	None	Focal peristrut deposits of acellular purple-staining material	Diffuse peristrut deposits	Central extension of deposits
Necrosis	None	Focal loss of nuclear staining	Up to 50% loss of nuclear staining	Full thickness involvement
Adventitial fibrosis	Normal thickness (<200 μm)	Focal increased thickness	Circumferential increased thickness (200 to 400 μm)	Circumferential increased thickness (>400 μm)

group A. QCA stent diameter and reference diameter did not differ among the dose groups. The model created oversized stent injury with stent/artery ratios averaging 1.21 to 1.28. There was dose-dependent improvement in all parameters of stenosis severity (MLD, mean diameter, maximum and mean percent stenosis, and late loss). MLD increased by 30%, 40%, and 90%, whereas mean late loss decreased by 37%, 56%, and 62% at 16, 22, and 29 Gy, respectively.

IVUS confirmed that stent area, diameter, and eccentricity did not differ among the dose subgroups. There was improvement in lumen area, intimal area, and percent area stenosis at each dose, but dose-dependent differences were less marked compared with QCA.

Injury score and histological stent area were similar between dose subgroups. There was substantial injury in all groups (injury scores 1.5 to 1.6). Lumen area, intimal area,

TABLE 2. QCA, IVUS, and Histological Parameters as Function of Dose for Group A

	Dose			
	Control	16 Gy	22 Gy	29 Gy
QCA				
n	8	8	8	8
Stent diameter, mm	3.4 \pm 0.4	3.2 \pm 0.4	3.2 \pm 0.3	3.4 \pm 0.3
Reference diameter, baseline, mm	2.8 \pm 0.3	2.5 \pm 0.3	2.5 \pm 0.2	2.7 \pm 0.3
MLD, mm	1.0 \pm 0.7	1.3 \pm 0.7	1.4 \pm 0.6	1.9 \pm 0.8*
Mean lumen diameter, mm	1.7 \pm 0.6	2.2 \pm 0.4*	2.5 \pm 0.4†	2.8 \pm 0.3‡
Diameter stenosis, %	61 \pm 26	45 \pm 31	39 \pm 28	23 \pm 31*
Diameter stenosis, mean, %	30 \pm 20	4 \pm 18†	-12 \pm 19‡	-13 \pm 12‡
Maximal late loss, mm	2.4 \pm 0.8	2.0 \pm 0.6	1.8 \pm 0.7	1.5 \pm 0.8*
Mean late loss, mm	1.6 \pm 0.7	1.0 \pm 0.2*	0.7 \pm 0.5‡	0.6 \pm 0.4‡
IVUS				
n	8	8	7	8
Lumen area, mm ²	4.4 \pm 1.2	7.2 \pm 1.8†	7.1 \pm 1.8†	7.6 \pm 1.6‡
Intimal area, mm ²	4.3 \pm 1.9	2.4 \pm 1.0†	2.3 \pm 1.4†	2.2 \pm 0.9†
Area stenosis, %	48 \pm 18	25 \pm 11†	25 \pm 17†	23 \pm 10†
Histomorphometry				
n	32	32	32	32
Injury score	1.6 \pm 0.4	1.6 \pm 0.5	1.5 \pm 0.6	1.6 \pm 0.5
Lumen area, mm ²	2.0 \pm 1.0	3.3 \pm 1.8†	3.6 \pm 1.8‡	5.0 \pm 1.8‡
Intimal area, mm ²	4.3 \pm 1.6	2.6 \pm 2.2†	1.9 \pm 2.1‡	1.5 \pm 1.9‡
Area stenosis, %	66 \pm 18	42 \pm 32‡	32 \pm 32‡	22 \pm 27‡
Intimal thickness, mean, mm	0.66 \pm 0.26	0.41 \pm 0.34†	0.31 \pm 0.33‡	0.23 \pm 0.28‡

Values are mean \pm SD.

* P <0.05, † P <0.01, and ‡ P <0.001 vs control.

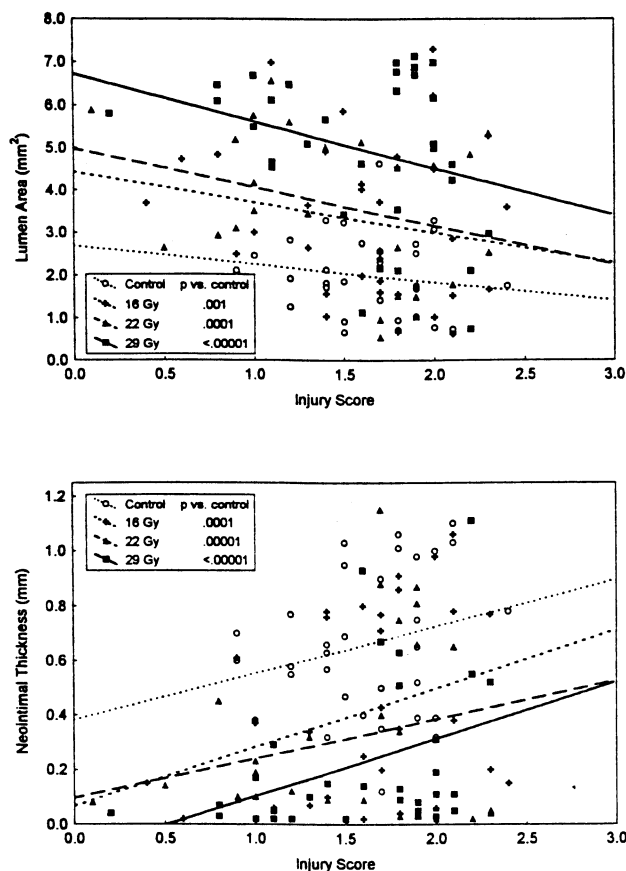


Figure 3. Scatterplots showing histomorphometric measurements of lumen area and neointimal thickness versus injury score for all group A sections. Intergroup post hoc testing probability value was by ANCOVA.

area of stenosis, and mean intimal thickness improved as a function of dose, with all radiation groups significantly different from control groups. At 29 Gy, there was a 150% increase in lumen area and a 67% decrease in stenotic area (22% versus 66% in controls). Similar radiation effects were seen in the LAD and RCA. Figure 3 plots neointimal thickness and lumen area as a function of injury score. ANCOVA testing showed that when injury-related effects were accounted for, the dose-dependent effects of radiation resulted in very strong statistical differences compared with controls ($P \leq 0.0001$ for all doses).

Irradiation After Stenting

Table 3 summarizes the quantitative analyses for group B. All parameters of stenosis severity improved with radiation, and most achieved statistical significance despite the small sample size. MLD and mean lumen diameter increased by 31% and 37%, respectively. The mean in-stent diameter remained 17% larger than the reference diameter, and mean late loss decreased by 54%. IVUS showed 50% and 62% decreases in intimal area and percent area stenosis, respectively. Histomorphometry yielded a 69% reduction in intimal area, a 170% improvement in lumen area, and a 67% decrease in stenotic area (21% versus 65% in controls).

TABLE 3. QCA, IVUS, and Histological Parameters as Function of Dose for Group B

	Dose	
	Control	29 Gy
QCA		
n	6	7
Reference diameter, baseline, mm	2.5±0.3	2.7±0.2
MLD, mm	1.3±0.4	1.7±0.8
Mean lumen diameter, mm	1.9±0.3	2.6±0.2*
Diameter stenosis, maximum, %	48±14	23±35
Diameter stenosis, mean, %	20±14	-17±18†
Mean late loss, mm	1.3±0.5	0.6±0.3‡
Maximum late loss, mm	1.9±0.5	1.4±0.8
IVUS		
n	6	7
Lumen area, mm ²	5.3±1.5	7.7±1.3†
Intimal area, mm ²	3.6±2.1	1.8±0.7‡
Area stenosis, %	34±22	13±9‡
Histomorphometry		
n	24	28
Injury score	1.8±0.3	1.7±0.3
Lumen area, mm ²	1.7±0.7	4.6±1.8*
Intimal area, mm ²	3.9±1.3	1.2±1.8*
Area stenosis, %	65±21	21±31*
Intimal thickness, mean, mm	0.66±0.26	0.23±0.28*

Values are mean±SD.

* $P < 0.001$. † $P < 0.01$, and ‡ $P < 0.05$ vs control.

Edge Effects

When groups A and B were combined, there was a significant difference in the distribution of angiographic stenosis location ($P=0.0002$). Of 14 control arteries, 11 (78%) had $\geq 50\%$ stenosis involving the entire stent, whereas only 3 (21%) had $< 50\%$ stenosis. Of 31 irradiated arteries, 2 (6%) had diffuse stenosis, whereas 8 (26%) had focal edge stenosis, and 21 (68%) had no stenosis (Figure 4). Of the 8 edge stenoses, 5 were distal, 2 were proximal, and 1 involved both edges. Also, in the edge stenosis cases, the stent/artery ratio was higher for the distal reference segment than for the proximal reference (1.46±0.28 versus 1.15±0.10, respectively; $P=0.013$).

Figure 5 shows serial pullback IVUS measurements. In controls, the entire stent length was narrowed relative to the proximal and distal reference segments. In irradiated vessels, all doses inhibited intimal thickening within the stent. At 16 Gy, however, there was a focal zone of narrowing adjacent and immediately distal to the stent ($P=0.003$ versus controls). Focal edge stenosis was approximately as severe as the worst in-stent narrowing in controls. The major cause was increased neointimal area ($P=0.002$), whereas no change in vessel size was observed. There was no edge stenosis with higher dose radiation.

Histological Effects

Figure 6 shows representative histology sections. Table 4 summarizes the scored histological features in group A.

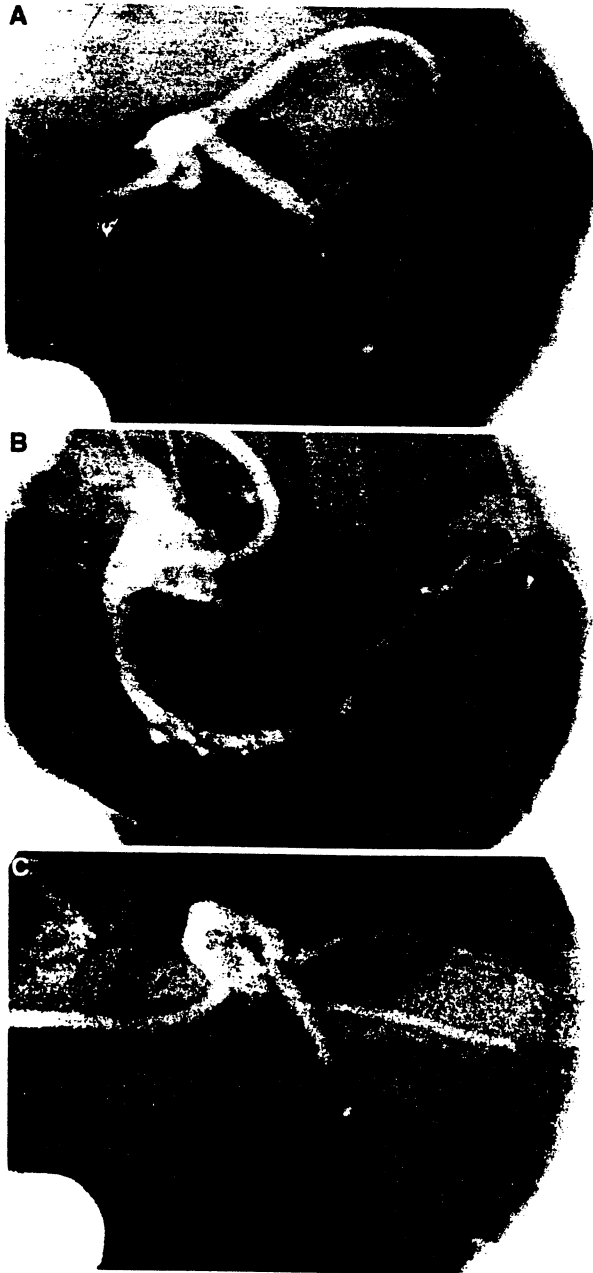


Figure 4. Angiographic examples. A, Control stent with diffuse in-stent restenosis. B, Sixteen Gy with distal edge stenosis. C, twenty-nine Gy with minimal late lumen loss.

Control vessel neointima was highly cellular and composed predominantly of smooth muscle cells and extracellular matrix. Radiation had a dose-dependent negative correlation with neointimal cellularity. At 29 Gy, the neointima was acellular and free of matrix in 18 (56%) of 32 sections. When cellular, the predominant cell type resembled control smooth muscle cells. The most striking effect of radiation was an increase in fibrin surrounding the struts ($P < 0.0001$). At 29 Gy, there was more medial absence and necrosis. The media was replaced with fibrin similar to the neointimal deposits. The adventitia also tended to be thicker in radiation-treated arteries. No differences were seen in the severity of the inflammatory response, and the vasa vasorum appeared

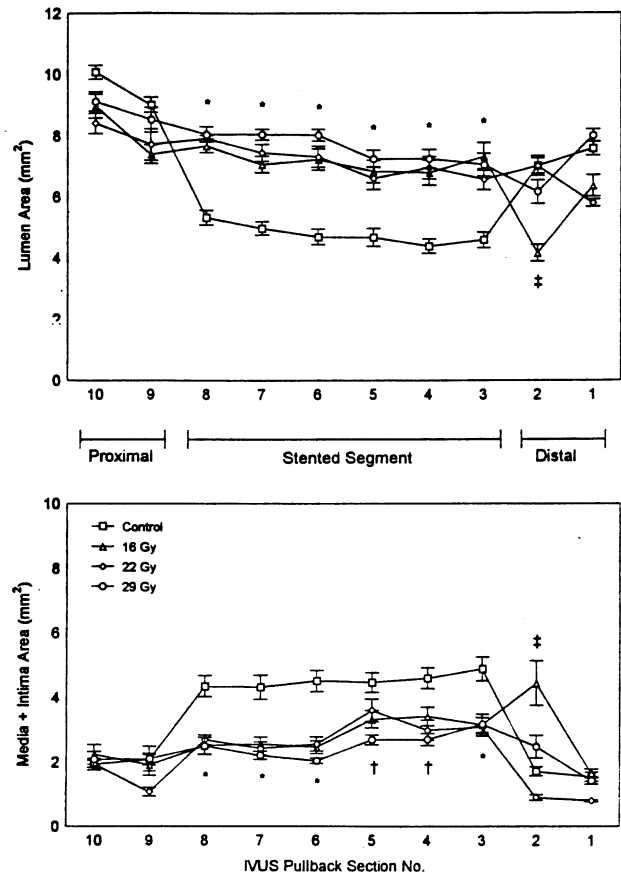


Figure 5. Graphs of lumen area and media+intima area during IVUS pullback. Sections are located at ≈ 2.5 -mm intervals. Data are shown as mean \pm SE. * $P < 0.05$ for all radiation doses vs control; † $P < 0.05$ for 29 Gy vs control; and ‡ $P < 0.005$ for 16 Gy vs control.

normal. The adjacent myocardium was free of fibrosis. Histological sections from group B control and irradiated vessels after 2 months were indistinguishable from respective group A sections. Sections 48 hours after radiation showed widely patent stents with circumferential acellular fibrin surrounding the struts and adhering to the adjacent vascular wall. Media was absent for 30% to 50% of the circumference consistent with balloon overstretch injury. The adventitia was thickened and contained diffuse infiltration with acute and chronic inflammatory cells.

Discussion

The present report evaluates a new liquid-filled ^{188}Re balloon system in a porcine coronary oversized stent injury model using 3 independent analytical tools: QCA, IVUS, and histomorphometry. Radiation before stenting produced a dose-dependent reduction of intimal thickening at 4 weeks. Improvement was documented in every index of lumen patency, whether measured as an absolute dimension or a ratio indexed to a reference diameter or area. There was a measurable effect at 16 Gy that improved stepwise with higher doses. At 29 Gy, the stenotic area improved from a control of 66% to 22%. These data are consistent with the previously reported experience of Waksman et al.⁴ albeit at different dose prescriptions.

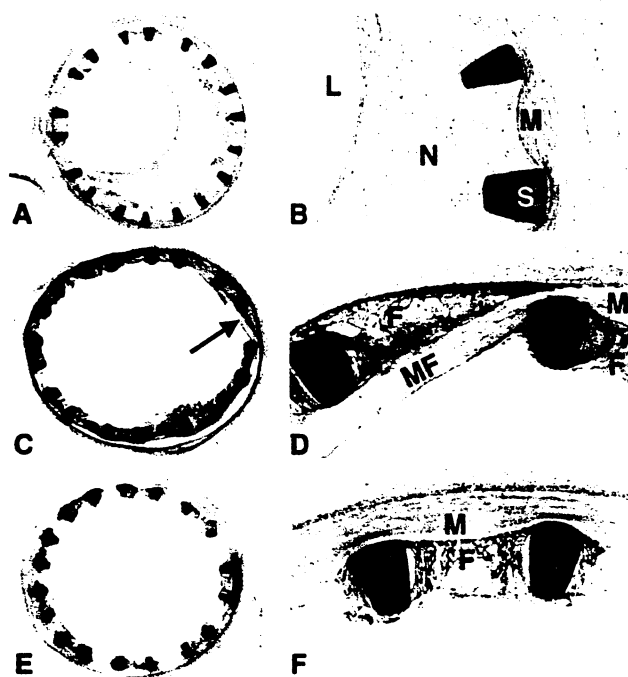


Figure 6. Photomicrographs of representative histological sections at original magnifications of $\times 10$ (A, C, E) and $\times 40$ (B, D, F). Stent struts are $\approx 180 \mu\text{m}$ thick. A and B, Stented control section at 60 days. There is an eccentric cellular neointima (N) with abundant extracellular matrix covering stent struts (S) reducing lumen (L) area. Media (M) is intact but is diffusely necrotic (nuclear dropout). C and D, Irradiated segment (29 Gy) at 2 days. Arrow indicates localized medial flap (MF). Darkly stained fibrinoid material (F) surrounds luminal side of each strut. Media has been disrupted or absent for $\approx 50\%$ of vessel circumference. E and F, Irradiated segment (29 Gy) at 60 days. There is abundant fibrin surrounding struts without cellular proliferation. Media is intact but with reduced nuclear staining.

Neointimal thickness was proportional to local mechanical injury in controls. When the effects of injury were accounted for by ANCOVA testing, the radiation was more statistically differentiated from controls. Radiation was effective over the

broad range of injury scores. Most irradiated sections had substantially less intimal thickening than did control sections; however, a minority of the irradiated sections were indistinguishable from the control sections, both morphometrically and histologically. We suspect that these irradiated proliferating segments received a lower dose because of the difficulty of positioning the 17-mm stent precisely in the middle of the 20-mm irradiated zone. This, along with the edge effects, may explain why maximum late loss was not reduced as impressively as mean late loss. Even so, the overall effects of radiation were strong, and the 3 analytical methods were in close agreement.

Irradiating after stent placement remains controversial. Wiedermann et al⁵ showed that irradiating after stenting was less effective by use of a γ source. Amols et al⁶ showed that the type of stent, its metallic composition, and design geometry modify dosimetry. In group B, radiation after stenting with a moderately radiopaque thick-walled stent did not interfere with the biologic effect. According to Figure 2, the actual dose to tissue at a depth 0.5 mm from the external surface of the stent was 23 Gy, or a 21% dose reduction due to stent attenuation and standoff thickness of 0.008 inches.

The histological signature of successful radiation therapy was persistence of neointimal fibrin from early after stenting (2 days) to 30 and 60 days after stenting. Radiation had no effect on inflammatory cell infiltration or foreign body reaction around the struts. The vasa vasorum and adjacent myocardium appeared normal. Other histological correlates of radiation were medial fibrin and adventitial thickening.

The ^{32}P Stent (Isostent) and the ^{90}Sr BetaCath (Novoste) have been associated with restenosis at the ends of the radiation zone, creating a candy wrapper-like appearance.^{7,8} There are data in balloon-injured porcine arteries showing that lower dose radiation may promote proliferation, thus suggesting that border zone restenosis may be secondary to insufficient dose.⁹⁻¹¹ The present study systematically evaluated the border zones by QCA and IVUS. With radiation, the smallest lumen diameter tended to be at the distal portion

TABLE 4. Ranked Histological Variables for Group A

Variable	Control	16 Gy	22 Gy	29 Gy	P	r
Neointima						
SMCs+matrix	2.19 \pm 0.64	1.37 \pm 1.21	1.03 \pm 1.20	0.59 \pm 0.98	<0.0001	-0.50
Inflammation	0.47 \pm 0.51	0.81 \pm 0.78	0.71 \pm 0.76	1.00 \pm 0.91	0.10	
Foreign body reaction	0.66 \pm 0.60	0.72 \pm 0.52	1.00 \pm 0.90	0.97 \pm 0.66	0.19	
Fibrinoid material	0.75 \pm 0.44	2.06 \pm 1.01	2.43 \pm 0.83	2.84 \pm 0.37	<0.0001	0.71
Media						
Fraction missing	0.16 \pm 0.14	0.18 \pm 0.15	0.24 \pm 0.13	0.31 \pm 0.17	0.0004	0.34
Necrosis	0.25 \pm 0.44	0.48 \pm 0.50	0.64 \pm 0.68	0.66 \pm 0.70	0.041	0.24
Fibrosis	0.00 \pm 0.0	0.0 \pm 0.0	0.07 \pm 0.26	0.12 \pm 0.34	0.055	0.23
Inflammation	0.03 \pm 0.18	0.03 \pm 0.18	0.14 \pm 0.36	0.34 \pm 0.06	0.26	
Adventitia						
Necrosis	0.00 \pm 0.00	0.00 \pm 0.00	0.00 \pm 0.00	0.03 \pm 0.09	0.41	
Fibrosis	0.78 \pm 0.75	1.28 \pm 1.02	1.6 \pm 1.06	1.43 \pm 1.01	0.009	0.26
Inflammation	0.72 \pm 0.68	0.84 \pm 0.85	0.71 \pm 0.94	0.77 \pm 0.50	0.75	

Values are mean \pm SD.

of the stents compared with diffuse in-stent restenosis seen in controls. Higher stent/artery ratios at the distal part of the stent may create more mechanical injury at the distal edge. At 16 Gy, a highly focal (<5-mm) segment just distal to the stent was significantly narrowed because of exaggerated intimal thickening. One hypothesis is that an insufficient radiation dose paradoxically enhances proliferation in the presence of severe vascular injury. These observations may also be an artifact of the short effective length of the irradiating balloon versus the stent (18 versus 17 mm) and any misalignment between these 2 zones. These data suggest that understanding the nature, severity, and mechanism of border zone phenomena will be an important area of future research.

Although the radiation delivery system was safe and efficacious in an animal model, there are several limitations that should lend caution to any inference about clinical efficacy. The porcine coronary model has no atherosclerosis, there was severe mechanical injury from oversized stenting, and the follow-up period was short. These considerations notwithstanding, a ^{188}Re balloon incorporates many of the features that may enhance the feasibility and potentially clinical efficacy compared with other brachytherapy systems. The high β energy and short half-life help achieve a low relative surface dose and short treatment times. At 150 mCi/mL, 3 to 6 minutes of inflation is required, depending on the balloon diameter. The γ emissions aid calibration and detection of picocurie-sized leaks with a Geiger counter. The isotope generator has a 2-month half-life and can be automated, and per-patient costs can be kept low. Waste management requires holding radioactive material for 1 week (10 half-lives) and then discarding it as biohazard waste. The primary advantages of a balloon-based system are precision dosimetry and ease of delivery. The source is centered with respect to the lumen, and the dose distribution is homogeneous in both axial and radial dimensions. Circumferential wall contact minimizes stent strut shadows, and IVUS dimensioning is not required to limit the dose to the nearest target.¹² The device is 6F guide catheter compatible and is applicable in small, distal, and tortuous vessels reachable with modern low-profile PTCA balloons.

Specific design features and methodology for use emphasize safety. Redundant seals prevent radiation leaks at the ISAT-catheter interface. The pressure-limiting valve restricts inadvertent overpressurization of the balloon to >4 SDs below the mean burst pressure of the balloon. The isotope has a short half-life, and urinary excretion can be enhanced by diuresis. Although perrhenate is concentrated 10- to 100-fold in the thyroid, stomach, large intestine, and bladder wall, treatment with oral perchlorate reduces these organ doses to average whole-body levels.^{13,14}

Preliminary experience with a ^{188}Re balloon intravascular brachytherapy device in a porcine coronary stent model suggests that radiation reduces restenosis in a dose-dependent fashion, as evaluated by QCA, IVUS, and histomorphometry. Radiation was equally effective when given before or after stent placement. Restenosis at the borders of the irradiated segment is a potential limitation. Persisting neointimal fibrin was associated with reduced cellular proliferation and matrix deposition. Radiation exposures were acceptable for day-to-day usage in the cardiac catheterization laboratory.

Acknowledgment

This study was supported by a grant from United States Surgical, Inc.

References

1. Kastrati A, Schömig A, Elezi S, et al. Predictive factors of restenosis after coronary stent placement. *J Am Coll Cardiol*. 1997;30:1428-1436.
2. Burns WA, Bretschneider AM, Morrison AB. Embedding in large plastic blocks: diagnostic light and potential electron microscopy on the same block. *Arch Pathol Lab Med*. 1979;103:177-179.
3. Schwartz RS, Murphy JG, Edwards WD, et al. Restenosis after balloon angioplasty: a practical proliferative model in porcine coronary arteries. *Circulation*. 1990;82:2190-2200.
4. Waksman R, Robinson KA, Crocker IR, et al. Intracoronary radiation before stent implantation inhibits neointima formation in stented porcine coronary arteries. *Circulation*. 1995;92:1383-1386.
5. Wiedermann JG, Marboe C, Amols H, et al. Intracoronary irradiation fails to reduce neointimal proliferation after oversized stenting in a porcine model. *Circulation*. 1995;92(suppl 1):I-146. Abstract.
6. Amols HI, Trichter F, Weinberger J. Intracoronary radiation for prevention of restenosis: dose perturbations caused by stents. *Circulation*. 1998;98:2024-2029.
7. Albiero R, Di Mario C, De Gregorio J, et al. Intravascular ultrasound (IVUS) analysis of b-particle emitting radioactive stent implantation in human coronary arteries: preliminary immediate and intermediate-term results of the Milan study. *Circulation*. 1998;98(suppl 1):I-780. Abstract.
8. King SB III, Klein JL, Bonan R, et al. The Beta Restenosis Trial: updated results and subgroup analysis. *Circulation*. 1998;98(suppl 1):I-651. Abstract.
9. Waksman R, Robinson KA, Crocker IR, et al. Endovascular low-dose irradiation inhibits neointima formation after coronary artery balloon injury in swine: a possible role for radiation therapy in restenosis prevention. *Circulation*. 1995;91:1533-1539.
10. Weinberger J, Amols H, Ennis RD, et al. Intracoronary irradiation: dose response for the prevention of restenosis in swine. *Int J Radiat Oncol Biol Phys*. 1996;36:767-775.
11. Giedd KN, Amols H, Marboe CC, et al. Effectiveness of beta-emitting liquid-filled perfusion balloon to prevent restenosis. *Circulation*. 1998;96(suppl 1):I-220. Abstract.
12. Teirstein PS, Massullo V, Jani S, et al. Catheter-based radiotherapy to inhibit restenosis after coronary stenting. *N Engl J Med*. 1997;336:1697-1703.
13. Kotzerke J, Fenchel S, Guhlmann A, et al. Pharmacokinetics of $^{99\text{m}}\text{Tc}$ -pertechnetate and ^{188}Re -perrhenate after oral administration of perchlorate: option for subsequent care after the use of liquid ^{188}Re in a balloon catheter. *Nucl Med Commun*. 1998;19:795-801.
14. Hausleiter J, Li A, Knapp FF, et al. Low body exposure in case of radioactive balloon leakage: a biodistribution and elimination study of ^{188}Re in pigs. *J Am Coll Cardiol*. 1999;33(suppl 2):44A. Abstract.